Engineered Science
DOI: https://dx.doi.org/10.30919/es1595

Dextrin/Polyvinyl Alcohol/Iodine Complexes: Preparation, Characterization, and Antibacterial, Cytotoxic Activity

Seitzhan Turganbay,[1,*] Alexander Ilin,[1] Aitugan Sabitov,[4] Dana Askarova,[1] Ardak Jumagaziyeva,[2] Zhanar Iskakbayeva,[2] Anar Seisembekova,[1] Tamara Bukeyeva[3] and Amir Azembayev[1]

Abstract

Bacterial infections have consistently posed a significant danger to public health. It is crucial to develop effective antibacterial agents from natural polymers. In this study, we propose a novel approach by combining dextrin and polyvinyl alcohol (PVA) to create an effective iodine delivery system with enhanced antimicrobial properties and biocompatibility, showing strong potential for wound management applications. Dextrin/PVA/iodine complexes were prepared by dissolving dextrin and PVA in water, followed by the addition of an iodine solution. The samples were characterized using ultraviolet–visible spectroscopy, Fourier transform infrared spectroscopy, proton nuclear magnetic resonance spectroscopy, and X-ray diffraction methods, confirming that the dextrin/PVA/iodine complexes were successfully prepared. Thermogravimetric (TG) analysis indicated that the chemical modification of dextrin and iodine complexation reduced the thermal stability; titration analysis revealed that 95% of the iodine in the dextrin/PVA/iodine complex was in the form of triiodide ions. The iodine contents of the three dextrin/PVA/iodine complexes (D/PVA/I-1, D/PVA/I-2 and D/PVA/I-3) were 4.27 ± 0.15%, 2.49 ± 0.18%, and 0.79 ± 0.21%, respectively. The antibacterial effects were evaluated *in vitro* against reference strains *Staphylococcus aureus* ATCC BAA-39, *Staphylococcus aureus* ATCC BAA-33591, *Streptococcus pneumoniae* ATCC BAA-660, *Escherichia coli* ATCC BAA-196, *Escherichia coli* ATCC BAA-2524, *Acinetobacter baumannii* ATCC BAA-1790, *Klebsiella pneumoniae* ATCC 700603, *Klebsiella pneumoniae* ATCC 2524 and clinical isolates *Streptococcus pneumoniae* SCAID PHRX1-2018, *Escherichia coli* SCAID WND1-2021, *Pseudomonas aeruginosa* SCAID PHRX1-2019 and *Pseudomonas aeruginosa* TA2. The results demonstrated that the dextrin/PVA/iodine complexes exhibited strong antibacterial activity against both reference and clinical strains, effectively inhibiting their growth. In particular, D/PVA/I-1 exhibited the best antibacterial effect. In a comparative analysis of the CTC50 of substances D/PVA/I-1, D/PVA/I-2 and D/PVA/I-3 using Tukey's multiple comparison test, no statistically significant differences were found among the groups. Therefore, CSAN-I complexes can be considered as promising candidates for wound management in clinical applications.

Keywords: Dextrin; Iodine; Polymer-iodine complex; Antimicrobial activity; Cytotoxic activity; Polyvinyl alcohol.
Received: 19 March 2025; Revised: 21 May 2025; Accepted: 13 June 2025.
Article type: Research article.

1. Introduction

Bacterial infections have long posed a significant public health threat due to their ability to cause widespread disease and death. To prevent chronic wound infections, antibacterial drugs (*e.g.*, antibiotics and antibacterial agents) are commonly used.[1] Despite their excellent antibacterial activities, these substances are highly cytotoxic, and their use is restricted by high production costs at the nanoscale and unstable chemical properties.[2,3] This threat has been exacerbated by the increase in antibiotic resistance emergence, which diminishes the effectiveness of treatments and complicates the management of common infections. The widespread resistance of clinically important pathogenic bacteria to available antibiotics has become a global problem due to the ever-increasing number of strains resistant to multiple antibiotics.[4,5] Therefore, the development of novel antimicrobial substances is urgently needed.

[1] *Laboratory of New Substances and Materials, JSC Scientific Center for Anti-Infectious Drugs, Almaty, 050060, Kazakhstan*
[2] *Laboratory of Microbiology, JSC Scientific Center for Anti-Infectious Drugs, Almaty, 050060, Kazakhstan*
[3] *Laboratory of Immunology, JSC Scientific Center for Anti-Infectious Drugs, Almaty, 050060, Kazakhstan*
[4] *Combustion Problems Institute, Nanobiotechnology Laboratory, Almaty, 050012, Kazakhstan*
**Email:* turganbay.s@gmail.com (S. Turganbay); aitugans@mail.ru (A. Sabitov)

Biopolymers are used in drug delivery systems due to their biocompatibility, biodegradability, and ability to protect and release therapeutic agents in a controlled manner. These materials can be engineered to improve the stability and solubility of drugs, target specific tissues or cells, reduce side effects, and enhance the overall efficacy of treatment.[6]

Dextrin, a polysaccharide derived from the hydrolysis of starch, is characterized by its high safety profile, non-toxicity, biocompatibility, and biodegradability.[7] Due to these advantageous properties, dextrin is widely employed across various fields, including the food industry, medicine, and tissue engineering.[8] Notably, its superior biocompatibility and wide range of properties, dextrin and its derivatives have been extensively studied as functional ingredients for various medical applications, particularly the prevention and treatment of bacterial infections in wounds.[9] Additionally, good solubility allows it to be used as a carrier for active components and antibacterial substances.

Poly(vinyl alcohol) (PVA) is well spread in biomedical applications due to its excellent biocompatibility, it functions as a stabilizer and is easily degradable, rendering it a suitable component for various medical formulations. Specifically, starch-PVA blends are utilized in drug delivery, taking advantage of PVA's ability to improve the stability, controlled release, and biodegradability of the drug delivery system. This combination enhances therapeutic efficacy, while minimizing potential side effects, making it a promising choice for the development of advanced biomedical materials.[10-12] Iodine exhibits potent antibacterial properties that affect various structures of microbial cells.[13] Due to its broad-spectrum antimicrobial activity, iodine has been extensively utilized for decades as a disinfectant and antiseptic.[14] More importantly, highly effective antibacterial iodine provides an alternative approach to lowering the possibility of high drug resistance of pathogenic microorganisms caused by antibiotic misuse.[15] The complexes formed by iodine and carrier feature high antibacterial activity, good stability, and low toxicity. In recent years, natural polymers have been employed for the incorporation of iodine, leading to the development of polymer-iodine composite materials, such as chitosan derivative-iodine microspheres and polysaccharide-iodine composite membranes, which demonstrate remarkable antibacterial activity.[16-19]

Classical studies by Makhayeva *et al*.[20] provided a detailed examination of the complexation mechanism between iodine and polyvinylpyrrolidone (PVP), demonstrating that complex formation involves charge transfer and results in a stable structure with antiseptic properties. Telfah *et al*.[21] showed that the degree of iodine incorporation and the stability of the resulting complexes vary depending on the nature of the polymer (*e.g.*, PEO, PVA, or polyurethanes), offering possibilities for tuning iodine release kinetics. Pesek *et al*.[22] analyzed the spectroscopic characteristics of iodine-polymer complexes, confirming that the complex structure influences optical properties, which can be exploited in analytical applications. Tashiro *et al*.[23] investigated the conductive properties of polymer–iodine complexes and demonstrated their potential applicability in organic electronics.

Furthermore, studies by Moulay *et al*.[24] emphasized the suitability of polymer–iodine complexes for developing controlled-release systems for active iodine, which is particularly relevant in the fields of medical materials and packaging. Collectively, these findings highlight the importance of polymer matrix selection and complexation conditions in designing materials with tailored functional properties. In this study, we propose a novel approach by combining dextrin and PVA to create an effective iodine delivery system with enhanced antimicrobial properties and biocompatibility, demonstrating high potential for wound management applications. The dextrin/PVA/iodine (D/PVA/I) complex was prepared by adding potassium iodide-iodine solutions to the polymer matrix, a semi-viscous medium capable of stabilizing and encapsulating iodine species formed of a homogeneous aqueous mixture of dextrin and PVA. The physicochemical properties and structures of the complexes were determined using various techniques, such as ultraviolet-visible (UV-Vis) spectroscopy, Fourier transform infrared (FTIR) spectroscopy, proton nuclear magnetic resonance (^{1}H NMR) spectroscopy, X-ray diffraction (XRD), and thermogravimetric analysis (TGA). Furthermore, *in vitro* antibacterial tests and cytotoxicity assays were used to evaluate the antibacterial activity and cytocompatibility of the dextrin/PVA/iodine complex, respectively. These findings lay the foundation for further development of the dextrin/PVA/iodine complex as a biomedical material for clinical applications.

2. Materials and methods

2.1 Materials

The reagents used for the present work were of analytical grade, obtained from commercial sources, and used without further purification. Potassium iodide from Sigma-Aldrich (St. Louis, MO, USA, ≥ 99%), iodine from Labpharm (JSC "Troitsky iodine plant", Russia, ≥ 98%), Dextrin (molecular weight ~4000 kDa and deacetylation degree of 95%) from Sigma-Aldrich (St. Louis, MO, USA, ≥ 99%), PVA from Sigma-Aldrich (molecular weight ~31000 kDa St. Louis, MO, USA, ≥ 99%), nutrient agar (Himedia, India), Tryptic Soy Agar (Himedia, India), Muller-Hinton Broth (Himedia, India), ampicillin sodium salt (Merck, Germany), sodium chloride >99% (*Mikhailovsky chemical reagents plant*, Russia), and ethanol (96% [Talgar Spirt', Kazakhstan]).

2.2 Test strains and growth conditions

The microorganisms used in this study were selected based on their clinical significance, multidrug resistance (MDR) profiles, and biofilm formation capacity. These characteristics are crucial in chronic and nosocomial infections. This allowed

for a comprehensive assessment of the antimicrobial efficacy of the tested compounds against both Gram-positive and Gram-negative bacteria. The test strains included both reference strains obtained from the American Type Culture Collection (ATCC, Rockville, MD, USA) and included multidrug resistant strains of bacteria. Some of the strains used in the experiment were obtained from their own museum collectionб were they deposited and patented as resistant strains. Gram-positive bacteria were presented by strains *Staphylococcus aureus* ATCC BAA-39, *Staphylococcus aureus* ATCC BAA-3359, *Streptococcus pneumoniae* ATCC BAA-660 and *Streptococcus pneumoniae* SCAID PHRX1-2018. ATCC BAA-196, *Escherichia coli* ATCC BAA-2524, *Escherichia coli* SCAID WND 1-2021 (patent #7713), *Pseudomonas aeruginosa* SCAID PHRX1-2019 (patent #6286), *Acinetobacter baumannii* ATCC BAA-1790, *Klebsiella pneumoniae* ATCC 700603, *Klebsiella pneumoniae* ATCC 2524 and clinical MDR isolate *Pseudomonas aeruginosa* TA2. Stock cultures were stored under the low temperature conditions at −80 °C. Before the experiments test strains were cultivated and twice passaged on Tryptic Soy Agar and Nutrient Agar as recommended in the ATCC handling information. The cells were incubated at 37 °C for 18-24 h.

2.3 Test system

Cytotoxicity of D/PVA/I-1, D/PVA/I-2 and D/PVA/I-3 was measured on two cell lines: MeT-5A (SV40 – immortalized human mesothelial cell line, ATCC-CRL-9444, USA) and MCF-7 (human breast adenocarcinoma, ATCC-HTB-22, USA). These cell lines are specifically produced for scientific laboratory studies. The cells proliferate efficiently at a cell area of 1×10^5 cells/cm^2, reaching 100% growth within two to three days of cultivation. The culture development was RPMI-1640 medium supplemented with 10% fetal bovine serum. The cells were cultured under the following conditions: 37 °C, 5% CO_2 and 95% humidity. Viability after cryopreservation ≥ 90% (trypan blue staining before culture). The source of cell cultures is ATCC. In addition, to determine D/PVA/I-1, D/PVA/I-2 and D/PVA/I-3 substances' toxic effect on immune cells, human peripheral blood mononuclear cells (Human peripheral blood mononuclear cells) were used as a test system.

2.4 Method of preparation of working solutions

2.4.1 Preparation of iodine-potassium iodide solutions

A total of 1.16 g of potassium iodide (KI) was weighed in a 100 mL glass flask and dissolved in 25 mL of purified water. The solution was left to cool to room temperature, 0.89 g of iodine (I_2) was added, the flask was stopped, and the flask was swirled until the iodine was completely dissolved.

2.4.2 Preparation of PVA Solution

A 100 mL glass flask was filled with 25 mL of distilled water preheated to 40 °C, after which 0.330 g of polyvinyl alcohol powder was added. Afterwards, the solution was thoroughly mixed.

2.5 Preparation of the dextrin/PVA/iodine complex

A 250 mL two-neck round-bottom flask was filled with 50 mL of distilled water and heated using a flask heater (LAB-FH-500 euro), while stirred. Once heated to 40 °C, a PVA solution was poured into the flask. The temperature was then gradually reduced to 25 °C, after which a potassium triiodide solution was introduced into the mixture. The resulting solution was thoroughly mixed for 10 minutes. The prepared sample was left in the flask for 12–24 hours to achieve equilibrium. The sample was dried under vacuum at a temperature of 40 ºC and stored in the dark for later use. To obtain complexes with different iodine contents, three dextrin/PVA/iodine complexes, labelled D/PVA/I-1, D/PVA/I-2, and D/PVA/I-3, were prepared by adjusting the molar ratio of the Dextrin, iodine and potassium iodide (D:I_2:KI =1.0:0.04:0.08, 1.0:0.02:0.04, and 0.004:0.008, respectively).

2.6 UV-Vis spectroscopy

UV-Vis spectra of the samples were collected using a LAMBDA-35 UV-Vis spectrophotometer (PerkinElmer, USA). The samples were dissolved in a water solution (1 mg/mL), and the solvent was used as a reference. The scanning range was 190-1100 nm.

2.7 FTIR spectroscopy

The samples were processed via the ZnS pellet method, and their FTIR spectra were collected using an FTIR spectrometer (Nicolet 6700 FTIR spectrophotometer, Thermo Scientific, USA). The test conditions were as follows: wavenumber range, 4000-400 cm^{-1}; scan number, 32; and resolution, 4 cm^{-1}.

2.8 ^{1}H NMR spectroscopy

^{1}H NMR spectra of the samples were collected using a superconducting Fourier NMR spectrometer JNM-ECA 500 (JEOL, Japan) operating at 500 MHz, and the solvent used was DCl/D2O (1/100, V/V).

2.9 XRD analysis

The samples were analyzed using an XRD diffractometer, SmartLab (Rigaku Ultima IV, Japan), under the following conditions: Cu Kα radiation (λ = 1.54059 Å), a one-dimensional detector (D/teX Ultra, Rigaku) with a Kβ filter, and step-scan measurements conducted within a 2θ range of 5-90°, with a step width (Δ2θ) of 0.1° and a scanning speed of 5°/min. Phase identification and investigation of the crystalline structure were performed using the PDXL: Integrated X-Ray Powder Diffraction Software and the international database ICDD PDF-2.

2.10 Thermogravimetric (TG) analysis

Thermal stability analysis of the samples was performed using

a TG/DSC STA 449 F1 Jupiter (NETZSCH, Germany) under the following conditions: nitrogen as the carrier gas, a flow rate of 50 mL/min, a temperature range of 30-600 °C, and a heating rate of 10 °C/min.

2.11 Determination of the iodine content

The concentration of halogens (iodine) in the complexes was measured by sodium thiosulfate titration.[25] The concentration of molecular iodine per 1000 g of the complex was measured by Eq. (1):

$$C_{I_2} = \frac{V_1 \cdot K_1 \cdot 12.69}{m} \quad (1)$$

where V_1 is the volume of 0.05 M sodium thiosulfate spent for complete titration; K_1 is the correction on sodium thiosulfate concentration in the buffer, for 0.05 M solution $K_1 = 0.5$; and m is the weight of the complex in g.

The concentration of KI was measured by Eq. (2) using titration with silver nitrate.[25]

$$C_{KI} = \frac{(V_2 \cdot K_2 - (V_1 \cdot K_1) \cdot 16.59}{m} \quad (2)$$

where V_1 is the volume of 0.05 M sodium thiosulfate spent for complete titration; V_2 is the volume of 0.05 M $AgNO_3$ spent for complete titration; and $K_1 = K_2 = 0.5$, m is the weight of the complex in g.

2.12 *In vitro* antimicrobial activity assay

Antimicrobial activity assay was performed using serial broth microdilution method according to the guidelines of the Clinical and Laboratory Standards Institute with some modifications.[26,27] The experiment was carried out in sterile 96-well polystyrene plates (BIOLOGIX, Jinan, Shandong, China).

(1) Serial two-fold dilution preparation: All the wells of the 96-well plate were filled with 100 µL of 0.9 % saline. Then 100 µL of samples was added into the first well in the raw of the plate. Further serial two-fold dilutions were performed: 100 µL of the saline+sample solution from the first well (A1) was mixed and transferred into the next well (A2) in the raw. 100 µL of the twice diluted solution from the second well (A2) was moved to the next well in the raw (A3) and so on, *etc*. until the required number of dilutions was achieved. All experiments were performed in triplicate.

(2) Cell suspension preparation and inoculation: The stock inoculum for each test-strain was prepared by the direct colony method: an aliquot of the test strain was taken with a bacteriological loop, transferred to a test tube with a sterile saline, and thoroughly homogenized until a homogeneous suspension was obtained. The density of the suspension of each studied strain was 0.5 units (according to McFarland), which corresponds to ~1.5×10^8 CFU/mL. To prepare the working suspensions of bacteria, the stock inoculum was diluted with saline 100 times to a final concentration of ~ 1.5×10^6 CFU/mL.

Thereafter, 10 µL of prepared bacterial suspensions were added into each well of the raw with test items. After 30 min incubation at 37 °C, 10 µL suspensions from each well were streak-plated onto nutrient agar/tryptic soy agar medium. The minimal bactericidal concentrations of iodine-containing compounds (MBCs) were determined as the lowest concentrations of the antimicrobial agent inhibiting culture growth after 30 min of incubation.

2.13 *In vitro* cytotoxicity assay

To determine the cytotoxic concentrations of the test substances, the cells (MCF7 and MeT-5A) were seeded in a 96-well plate at a concentration of 3×10^4 cells/unit and left for 24 hours in a CO_2 incubator (except for mononuclear cells, they were seeded in wells at a concentration of 1×10^5 cells/unit). After 24 hours, the medium was replaced with a fresh medium containing the test substances of the following concentrations: 5.0, 2.5, 1.25, 0.625, 0.312, 0.156, 0.078, 0.039 and 0.019 mg/ml. Each concentration rate was used thrice. RPMI-1640 medium was used as a diluent. The duration of exposure of the cells to the test substances was 48 hours in a CO_2 incubator. The negative control consisted of cells without the addition of the test substances.

The arithmetic mean value of optical density (OD) () for the concentration of each test substance was calculated using Eq. (3).

$$\bar{Y} = \frac{y_1 + \ldots + y_n}{n} = \frac{1}{n}\sum_{i=1}^{n} y_i \quad (3)$$

where y_i is the result of measuring the OD for each object in the group; n is the number of objects in the group.

The percentage of viability for each replicate of each concentration of the test substance was calculated using Eq. (4).

$$\%\, Viability = \frac{Y_i}{\bar{Y}_{NC}} \times 100\,\% \quad (4)$$

where Y_i is the result of OD measurement for each group; $\bar{Y}$NC is the arithmetic mean value of OD ($\bar{Y}$) for the negative control.

The standard deviation and percentage of viable cells for each concentration of the test substance were calculated using Eq. (5).

$$StD = \sqrt{\sum_{i=1}^{n}(Y_i - \overline{Y})^2/(n-1)} \quad (5)$$

2.14 3-(4,5-dimethylthiazol-2-yl)-2,5-diphenyltetrazolium bromide (MTT) assay

Cytotoxicity analysis was performed using the MTT method. This method for determining cell viability is based on the ability of living cells to convert soluble yellow 3-(4,5-dimethylthiazol-2-yl)-2,5-tetrazolium bromide into insoluble purple-blue intracellular formazan crystals. Nonviable dead

Table 1: Physicochemical properties of the dextrin/PVA/iodine complexes.

No	Name of indicators	Results		
		D/PVA/I-1	D/PVA/I-2	D/PVA/I-3
1	Empirical formula		$[C_8H_{14}O_6{\cdot}I_3]_n$	
2	Molecular weight, g/mol		587 g/mol	
3	pH	4.76	4.71	4.96
4	Solubility in water, g/100 mL	20 g (at 25 °C)	20 g (at 25 °C)	20 g (at 25 °C)
5	Melting temperature (°C)	172 (143-145)	182 (128-134)	194 (106-110)
6	Colour	Dark brown	Dark brown	Dark brown
7	Iodine content, (%)	4.27	2.49	0.79
8	Viscosity, mm^2/s	12.06	4.50	1.14
9	Density, g/cm^3	1.065	1.028	0.993
10	Yield (%)	95	95	96

cells do not have this ability. Four hours before the end of the studied drugs action, a 5 mg/ml MTT solution was added to the cultured cells. The cells were then cultured for the remaining 4 hours in a CO_2 incubator at 37 °C, 5% CO_2 and 95% humidity. After removing the culture medium, the formazan crystals were dissolved in 100 µl DMSO for 10 min. The amount of formazan crystals increases in direct proportion to the number of viable cells. The OD of dissolved formazan was measured using a Sunrise RC.4 microplate reader at 540/620 nm.[28]

3. Results and discussion

3.1 Physicochemical properties of the dextrin/PVA/iodine complexes

Dextrin/PVA/iodine complexes are solutions of a complex iodine compound with polydentate ligands, represented by carbohydrate and polymer associates. The active substance of the sample is an iodine-polymer complex, which serves as a matrix from which the active molecule iodine is gradually released. The colour, percentage yield and melting points (M.P) or temperature of decomposition (d) of the *dextrin/PVA/iodine complexes* are presented in Table 1. The complex was dark brown in color. The solubility of the *complexes* in water was determined by the Flask method (to determine values above 0.01 g/L) according to the OECD guidelines for the testing of chemicals (water solubility).

3.2 UV-Vis spectral analysis

The UV-Vis spectra of dextrin, PVA, and dextrin/PVA/iodine complexes are shown in Fig. 1. In the scanning range, the absorption peak of dextrin was located at ~278 nm, which is attributed to the n–π transition of heteroatoms (such as oxygen) in the dextrin molecule. The n–π transition requires relatively low energy, resulting in a weak absorption band at ~278–279 nm, which is consistent with the findings of Zhanguang Chen *et al.*[29] In the UV-Vis spectrum of PVA, three absorption peaks were observed at 207 nm, 279 nm, and 327 nm. These bands are assigned to n→π and π→π transitions, respectively. The n→π transition is likely due to the C=O groups, while the π→π transitions can arise from unsaturated bonds, such as C=C or conjugated C=O, possibly originating from residual acetate or oxidation byproducts at the terminal or side groups of PVA chains. In the spectrum of the dextrin/PVA/iodine

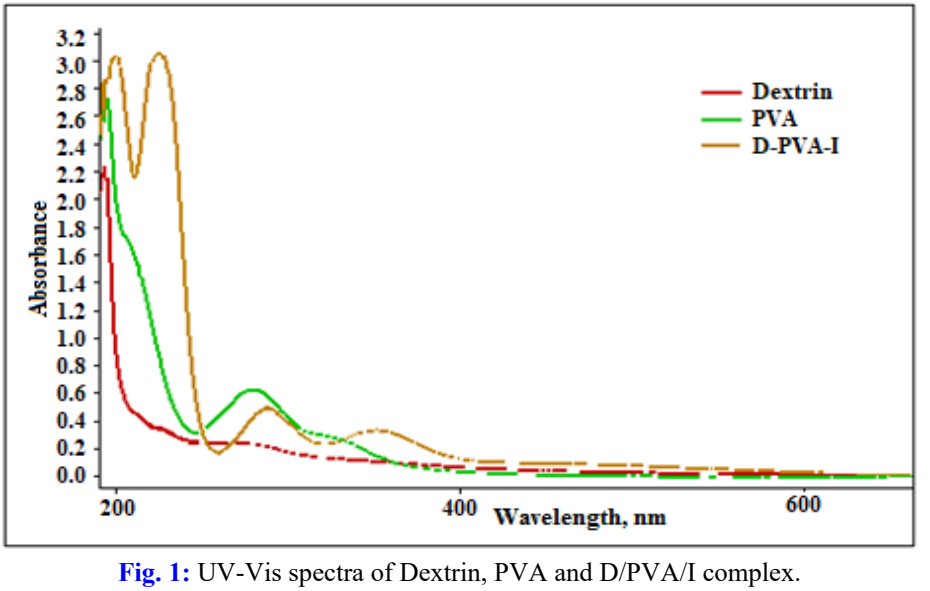

Fig. 1: UV-Vis spectra of Dextrin, PVA and D/PVA/I complex.

complex, three new absorption peaks appeared at 199 nm, 287 nm, and 351 nm. These peaks are attributed to the presence of molecular iodine (I_2) and triiodide ions (I_3^-), which are known to exhibit strong charge-transfer transitions in this region. These findings are consistent with the results reported by Sai *et al.*,[30] such absorption features are characteristic of I_3^- complexes and support the successful formation of a charge-transfer complex between iodine and the polymer matrix.

3.3 FTIR spectral analysis

The largest mass fraction in the dextrin/PVA/iodine complex is occupied by dextrin. In this regard, to clarify the interaction of the complex components, it is relevant to trace the changes occurring in the spectrum of dextrin in the final complex. Fig. 2 shows the IR spectra of dextrin, PVA, and dextrin/PVA/iodine. As shown in Fig. 2 (b), the bands at 3312 and 2925 cm^{-1} of free dextrin are attributed to the O-H stretching vibration and C-H stretching of the -CH_2 group, respectively. The peak at 1646 cm^{-1} is attributed to the wide intense band at C=C.[31-35] Moreover, the peaks at 1417 and 1336 cm^{-1} are related to the bending vibrations of the CH_3 and CH_2 groups,[31,32,36,37] and the peaks at 1146, 1076 and 994 cm^{-1} are related to the stretching vibrations of the C-O-C glycoside bond and the stretching vibrations of the C-O bonds.[31-34] The peak at 928 cm^{-1} is related to ring bond vibrations, and the peaks at 857 and 761 cm^{-1} are related to bending vibrations outside the plane of CH. [31,32,35]

In the spectrum of PVA, the large bands observed between 3332 cm^{-1} are linked to the stretching of O–H from intermolecular and intermolecular hydrogen bonds. The vibrational band observed at 2916 cm^{-1} refers to the stretching of C–H bonds from alkyl groups. The vibration bands at 1732, 1430, 1374, 1243, 1086 and 837 cm^{-1} corresponded to the stretching vibration, C=O carbonyl stretch, C–H bending vibration of CH_2, C–H deformation vibration, symmetrical stretching vibrations of the ring, C–O stretching of acetyl groups and C–C stretching vibration, respectively.[38-40]

Compared to those of dextrin, the spectra of the dextrin/PVA/I samples show that the most intense bands in both spectra correspond to C-O bonds. However, there is a noticeable shift in the wavenumbers. For dextrin, the wavenumber was 994 cm^{-1}, while in the complex, it shifted to 1016 cm^{-1}. Shifts are also observed in other less intense bands. After the most intense peak in the dextrin spectrum, bands with wavenumbers of 925, 857, and 761 cm^{-1} are present. In the spectrum of the complex, the corresponding bands shifted to 923, 850, and 767 cm^{-1}. These results demonstrate the complexation of iodine with dextrin.

3.4 ^{1}H NMR characterization

^{1}H NMR spectroscopy has proven to be an invaluable method for investigating the subtle structural differences in polymeric materials. The ^{1}H NMR spectra of Dextrin, PVA and Dextrin/PVA were shown in Fig. S1. In the ^{1}H NMR spectrum of dextrin, the anomeric proton of the glucose unit (H1) appears downfield at 5.244 ppm. Protons attached to carbons C2–C6 of the glucose units are observed in the range of 3.1–3.7 ppm, with specific signals at 3.102, 3.253, 3.472, 3.610, and 3.668 ppm. A methylene group (CH_2) associated with the branching point is detected at 3.796 ppm. Additionally, a weak signal from the hydroxyl group (OH) is observed at 5.067 ppm. These findings align with previously reported data.[41] the ^{1}H NMR spectrum of polyvinyl alcohol (PVA), several characteristic peaks are observed. The protons on the carbon attached to the hydroxyl group (–CH_2OH) appear in the range of 3.2-4.0 ppm (3.555, 3.699, and 3.869 ppm). The proton in the methylene group attached to the main chain carbon (–CH_2–CH–) is observed between 1.4-2.0 ppm (1.429, 1.475, 1.540,

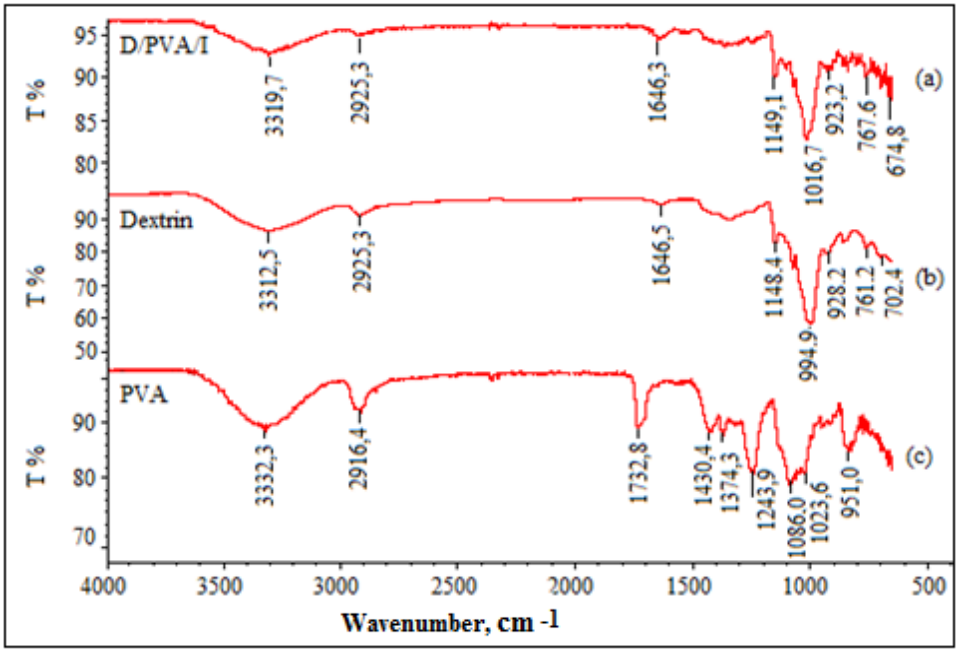

Fig. 2: IR spectra of dextrin (a), PVA (b), and dextrin/PVA/iodine (c)

1.756, and 1.938 ppm), with slight variations due to the polymer's structure and molecular weight. A methylene proton associated with the carbon at C_3 ($C–CH_2$) is detected at 3.183 ppm. Incomplete hydrolysis would show protons near the acetate group in the 2.1-2.4 ppm range, but in this sample, complete hydrolysis occurred, and no residual acetate groups are visible. Hydroxyl protons (−OH) are seen as a broad signal at 5.087 ppm. These results confirm the structure of PVA and its complete hydrolysis.

Comparison of the NMR spectra of dextrin, PVA, and their mixture with iodine and potassium iodide reveals distinct changes in chemical shifts and signal intensities, particularly in the 3.5-5.5 ppm region, indicating interactions between the components. In the spectrum of the mixture, signal broadening and shifts are observed, suggesting alterations in electron density within hydroxyl and ether groups, likely due to hydrogen bonding and complexation with iodine. These spectral changes confirm that iodine and potassium iodide interact with dextrin and PVA, forming a stable polymer-iodine complex, which may result from both physical adsorption and chemical bonding through donor-acceptor interactions.

3.5 XRD analysis

The crystal structure of dextrin, PVA and the structural changes in its complexes with iodine were probed using an X-ray diffractometer, and the XRD patterns were presented in Fig. 3. In the XRD patterns of dextrin, a characteristic broad hump was observed in the range of 2θ = 15-30°, indicating an amorphous structure. The typical diffraction peak associated with the (020) crystallographic plane appeared as a broad feature, suggesting that dextrin exists in an amorphous state. These findings are consistent with previously reported data.[42,43] The XRD pattern of PVA reveals two distinct peaks at 20.5° and 42.6°, which are indicative of the semi-crystalline nature of the PVA membrane.[44] The semi-crystalline structure of PVA is stabilized by both intramolecular and intermolecular hydrogen bonding.[45] In the D/PVA/I sample, the peak in the 19–20° 2θ region becomes broader and less pronounced, indicating a reduction in crystallinity due to the interaction of the components. This confirms the formation of a polymer-iodine complex, in which iodine destabilizes the crystalline regions of PVA, promoting greater structural amorphization.

3.6 TG analysis

According to the TG curves (Fig. 4a), the thermal decomposition behavior of the samples can be roughly divided into three stages at a constant heating rate of 10 °C/min. During the first stage, mass loss was observed between 28 and 150 °C for D/PVA/I-1 (5.9%), between 28 and 169 °C for D/PVA/I-2 (9.4%), and between 28 and 175 °C for D/PVA/I-3 (8.3%). This may be attributed to moisture loss, indicating that the complexes were not entirely anhydrous. The second stage, between 150 and 280 °C, corresponds to the glass transition of the samples, with mass losses of 22.6%, 28.8%, and 31.8% for the three complexes, respectively. In the third stage (218–600 °C), the TG curves sharply decreased, which was attributed to the cleavage of substituents and the depolymerisation of polysaccharide chains. In this stage, the mass losses were 24.46% for D/PVA/I-1, 22.49% for D/PVA/I-2, and 18.72% for D/PVA/I-3. The residual mass percentage recorded for D/PVA/I was 40.0%.

According to the differential thermal gravimetric (DTG) curves (Fig. 4b), the peak temperature indicates the rate of fastest mass loss for the sample at that temperature. The peak

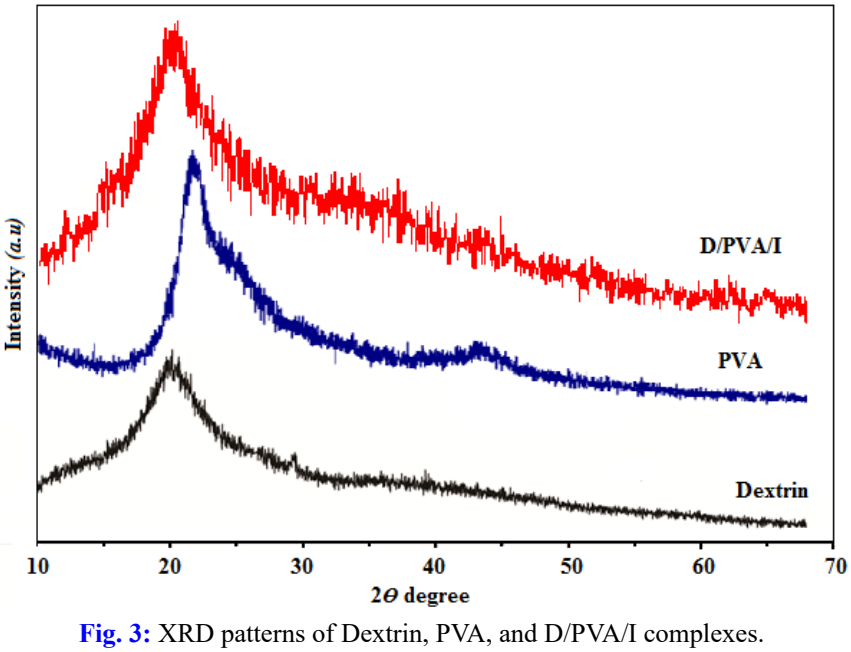

Fig. 3: XRD patterns of Dextrin, PVA, and D/PVA/I complexes.

temperatures for mass loss associated with dextrin dehydration were 74 and 85 °C, suggesting that dextrin has a high affinity for water and requires more energy to vaporize water molecules. The onset decomposition temperature of dextrin was 306 °C, while those of D/PVA-I-1, D/PVA-I-2, and D/PVA-I-3 were 160, 171, and 187 °C, respectively. Furthermore, the peak decomposition temperature of dextrin was 314 °C, and those of D/PVA-I-1, D/PVA-I-2, and D/PVA-I-3 were 172, 182, and 194 °C, respectively. These results suggest that the chemical modification of dextrin and its complexation with iodine led to a decrease in thermal stability due to the local amorphization of the crystalline structure of dextrin. To ensure the stability of the complexes, all technical operations should be carried out at temperatures below 160 °C.

Based on the results of UV-Vis spectroscopy, FTIR spectroscopy, ^{1}H NMR spectroscopy, XRD analysis, and thermogravimetric analysis, the structural formula of the dextrin/PVA/iodine complex has been proposed, as illustrated in Fig. 5.

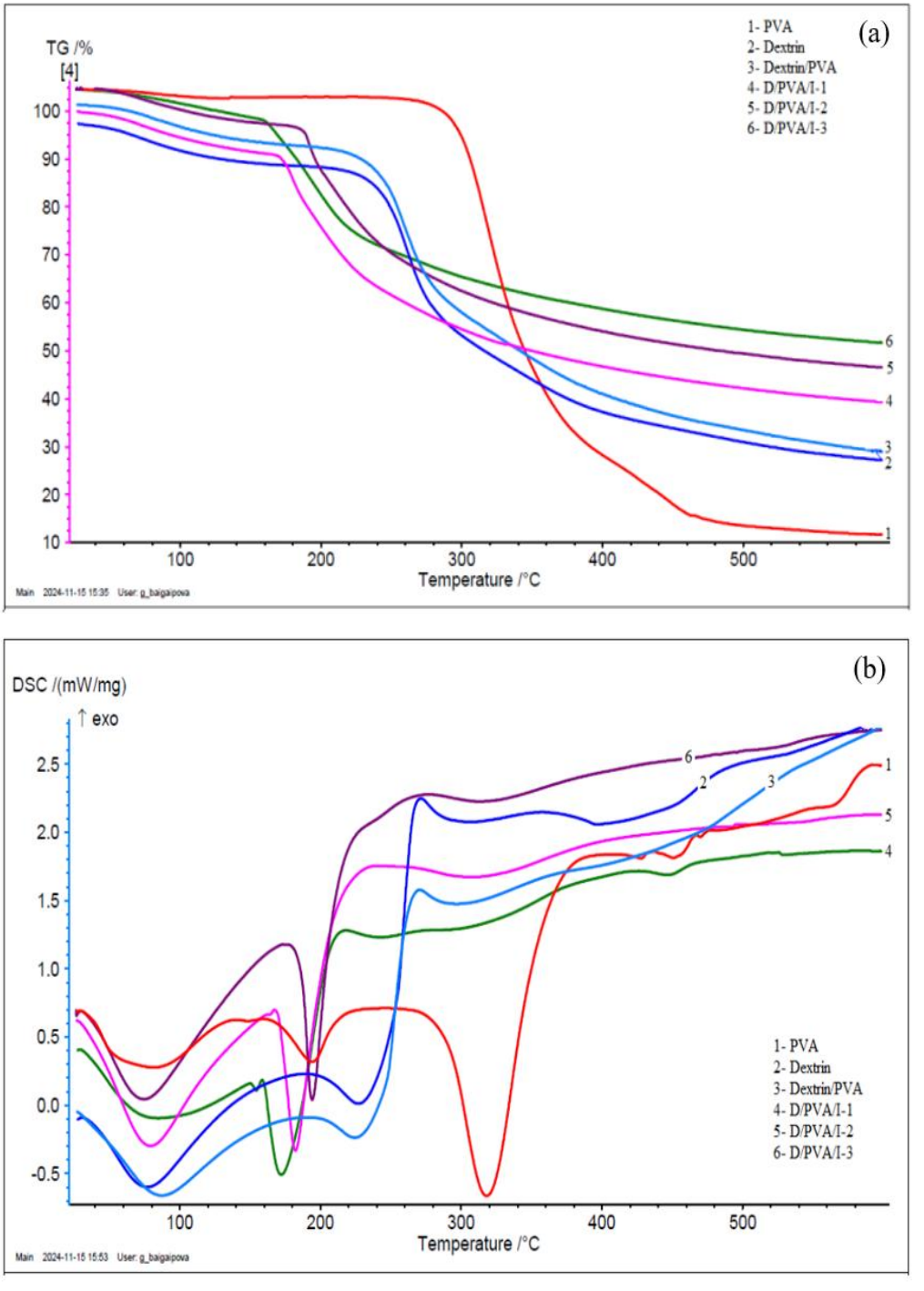

Fig. 4: (a) TG analysis curve and (b) DSC analysis curve of D/PVA/I complexes.

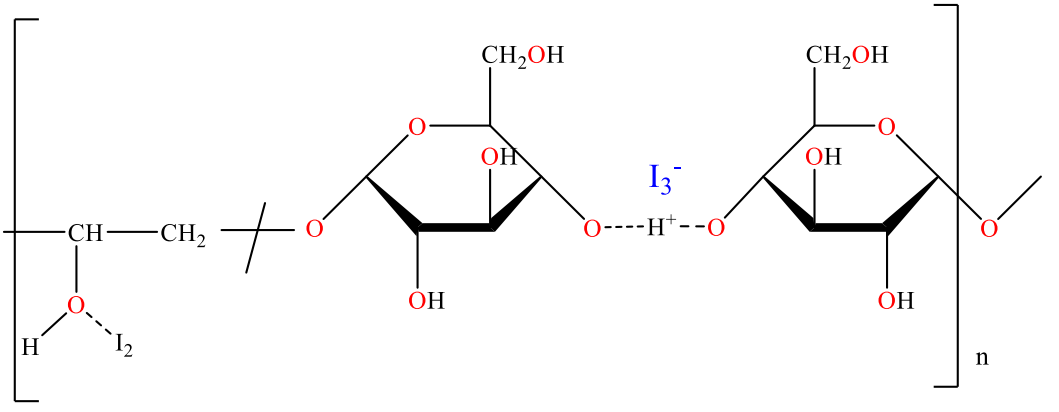

Fig. 5: The structure of Dextrin/PVA/I complex.

3.7 Antibacterial effect

The emergence of MDR pathogens poses a significant challenge to public health, leading to limited therapeutic options and increased mortality rates. In this context, our D/PVA/I complexes offer a promising alternative. Iodine-containing polymeric systems have demonstrated efficacy against MDR strains, including *S. aureus* and *E. coli*. Notably, the iodine-containing nano-micelle FS-1 has been shown to revert antibiotic resistance in *S. aureus* by inducing oxidative stress and destabilizing resistance-conferring genomic elements.[46] Furthermore, iodine-based materials have been effective in managing biofilm-associated infections, which are often resistant to conventional antibiotics. The D/PVA/I complexes, with their controlled iodine release, may provide sustained antimicrobial activity, addressing both planktonic and biofilm-forming bacterial populations.[47]

The incorporation of iodine into polymer matrices not only enhances antimicrobial efficacy but also offers stability and controlled release, making these complexes suitable for various clinical applications, including wound dressings and implant coatings. The antibacterial activity of samples D/PVA/I-1, D/PVA/I-2 and D/PVA/I-3 were tested by the two-fold dillution test against Gram-positive and Gram-negative bacteria. The test results are illustrated in Table 2.

The provided table presents the mminimum bactericidal concentration (MBC) values, expressed in micrograms per milliliter (μg/mL), for a series of bacterial strains subjected to different formulations, designated as D/PVA/I-1, D/PVA/I-2, and D/PVA/I-3. These formulations represent variations in the iodine (I_2) content relative to the total concentration of the substance, with each formulation exhibiting distinct antibacterial properties based on its iodine concentration. The MBC value is defined as the lowest concentration of the substance required to completely inhibit bacterial growth, making it an essential metric for evaluating antimicrobial efficacy.

Table 2 shows that the minimum bactericidal concentrations (MBCs) of the D/PVA/I complexes increase significantly from D/PVA/I-1 to D/PVA/I-3 across all tested bacterial strains. D/PVA/I-1 exhibits the highest antimicrobial activity (lowest MBC values), while D/PVA/I-3 demonstrates markedly reduced efficacy, particularly against Gram-negative bacteria such as *E. coli, K. pneumoniae*, and *P. aeruginosa* (MBCs reaching up to 21.6 μg/mL).

This trend is closely linked to the structural properties and iodine availability within the complexes. D/PVA/I-1 likely contains iodine in a more labile or diffusible form, perhaps due to weaker interactions between iodine and the polymer matrix, facilitating greater bioavailability. In contrast, D/PVA/I-3 may possess a denser or more crosslinked PVA structure, which could sequester iodine more tightly, reducing its release and thereby diminishing antimicrobial potency.

The disparity in activity between Gram-positive and Gram-negative strains further supports this, as the outer membrane of Gram-negative bacteria provides an additional diffusion barrier, amplifying the importance of iodine release kinetics. Notably, S. aureus and S. pneumoniae remain susceptible even to D/PVA/I-2, while Gram-negative strains show a sharper decline in sensitivity.

For *Staphylococcus aureus* strains (ATCC BAA-39 and ATCC BAA-33591), both D/PVA/I-1 and D/PVA/I-2 exhibit high MBC values (0.33 μg/mL and 0.68 μg/mL, respectively), demonstrating strong antibacterial activity. However, the formulation with lower iodine concentration (D/PVA/I-3) shows a significantly lower MBC (10.68 μg/ml). This suggests that higher iodine concentrations are more effective against *Staphylococcus aureus*, which is consistent with the literature data that emphasizes iodine's ability to disrupt cell wall synthesis and protein functions in Gram-positive bacteria.[48] The observed decrease in bactericidal activity with the lower iodine concentration in D/PVA/I-3 may indicate that a critical threshold of iodine is required to effectively combat *Staphylococcus aureus*.

Similarly, for Escherichia coli (ATCC 196, ATCC 2523 and SCAID URN 1-2020), the MBC values increase with decreasing iodine concentrations. The MBC for D/PVA/I-1 is 0.68 μg/mL, doubling for D/PVA/I-2 (1.34 μg/mL), and dramatically escalating to 21.6 μg/mL for D/PVA/I-3. This trend suggests that iodine concentration plays a crucial role in enhancing the bactericidal efficacy against Gram-negative

Table 2: MBC values of samples against test-strains.

Strains	D/PVA/I-1	D/PVA/I-2	D/PVA/I-3
	MBC values, μg/mL (I_2 Content Concentration per Total Concentration of the Substance)		
S. aureus ATCC BAA-39	0.33	0.68	10.68
S. aureus ATCC BAA-33591	0.33	0.68	10.68
E. coli ATCC 196	0.68	1.34	21.60
E. coli ATCC 2523	0.68	1.34	21.60
E. coli SCAID URN 1-2020	0.68	1.34	21.60
K. pneumoniae ATCC 700603	0.68	2.67	21.60
K. pneumoniae ATCC 2524	0.68	2.67	21.60
P. aeruginosa TA2	0.68	1.34	21.60
P. aeruginosa WND 1-2022	0.68	0.68	21.60
A. baumannii ATCC 1790	0.33	0.33	10.68
S. pneumoniae ATCC 660	0.33	0.33	10.68
S. pneumoniae SCAID PHRX 1-2018	0.68	0.68	10.68

bacteria such as E. coli. This finding aligns with existing studies that indicate iodine-based formulations are highly effective against E. coli, likely due to iodine's oxidative effects on the cell membrane and bacterial DNA.[49]

For *Klebsiella pneumoniae* strains, the MBC values follow a similar trend, increasing from 0.68 μg/mL (D/PVA/I-1) to 2.67 μg/mL (D/PVA/I-2), and reaching 21.6 μg/mL for D/PVA/I-3. This suggests that while the higher iodine concentrations provide better bactericidal performance, the lower iodine concentration in D/PVA/I-3 is significantly less effective against this pathogen. These results are consistent with literature reports that *Klebsiella pneumoniae* can be more resistant to lower concentrations of iodine due to its thicker outer membrane, which may reduce the penetration of iodine.[50]

Remarkably, the MBC values for *Pseudomonas aeruginosa* (TA2 and WND 1-2022 strains) remain relatively stable across D/PVA/I-1 and D/PVA/I-2, with values around 0.68 μg/mL, respectively. However, there is a significant decrease in MBC for D/PVA/I-3 (21.6 μg/mL). This suggests a possible tolerance or resistance mechanism in *Pseudomonas aeruginosa* at higher iodine concentrations, which has been previously reported in the literature.[51] The resilience of *P. aeruginosa* to iodine may be attributed to its robust efflux pumps or the production of biofilms that limit iodine penetration.[52]

For *Acinetobacter baumannii* and *Streptococcus pneumoniae* (ATCC 660 and SCAID PHRX 1-2018), the MBC for D/PVA/I-1 and D/PVA/I-2 is relatively high (0.33 μg/mL), and it decreases to 10.68 μg/mL for D/PVA/I-3. This finding is in line with the literature suggesting that Streptococcus pneumoniae is generally sensitive to iodine-based compounds.[53]

The observed trends in the MBC values of your D/PVA/I complexes align with findings from other studies on iodine-containing polymeric systems. For instance, research on PVP-iodine complexes has demonstrated their efficacy against both Gram-positive and Gram-negative bacteria, with the degree of crosslinking influencing the release rate and, consequently, the antimicrobial activity. Similarly, studies on controlled-release iodine foam dressings have highlighted the importance of iodine availability in combating biofilm formation and bacterial growth.[54-56] These studies suggest that the structural characteristics of iodine-polymer complexes, such as crosslinking density and iodine release kinetics, play a crucial role in determining their antimicrobial efficacy. The higher MBC values observed in your D/PVA/I-3 complex may be attributed to a more tightly bound iodine structure, leading to slower release rates and reduced antibacterial activity.

The antimicrobial action of iodine is primarily due to its ability to penetrate bacterial cell walls and disrupt cellular processes. In polymer-iodine complexes, the release of iodine is influenced by the polymer's structure and the nature of the iodine-polymer interaction. For example, in PVP-iodine complexes, iodine is coordinated with the nitrogen atoms of the pyrrolidone rings, and the release rate can be modulated by adjusting the degree of crosslinking.[56]

In the D/PVA/I complexes, variations in iodine content and polymer crosslinking likely affect the release dynamics, with D/PVA/I-1 exhibiting the most rapid iodine release and, consequently, the highest antimicrobial activity. The slower release in D/PVA/I-3 may result in suboptimal iodine concentrations at the bacterial cell surface, leading to diminished efficacy.

3.8. Evaluation of cytocompatibility

The cytotoxicity of D/PVA/I-1, D/PVA/I-2 and D/PVA/I-3 substances was determined by the viability of MCF7, MeT-5A

and human PBMC cells using the MTT method. The cytotoxicity of D/PVA/I-1, D/PVA/I-2, and D/PVA/I-3 was determined by the viability of MCF7, MeT-5A, and PBMC human cells using the MTT assay. The results of the studies of D/PVA/I-1 showed moderate toxicity to the MCF7 tumor line at a concentration of 5 mg/mL (62.4% viable cells) and to PBMC at concentrations of 5 and 2.5 mg/mL (52.0% and 56.6% viable cells, respectively), while a dose-dependent effect was observed in PBMC. In the case of the normal MeT-5A cell line, D/PVA/I-1 at concentrations of 5.0 mg/mL and 2.5 mg/mL resulted in a pronounced toxic effect on the cells (13.8% and 23.0% viable cells, respectively), as shown in Fig. 6.

Studies of D/PVA/I-2 showed that moderate toxicity was observed with respect to PBMC (61.5% viable cells) when exposed to a concentration of 5.0 mg/mL, and pronounced toxicity was observed with respect to the normal MeT-5A cell line (47.0% viable cells). No pronounced toxic effect was shown with respect to the MCF7 tumor line when exposed to D/PVA/I-2, as shown in Fig. 7. Substance D/PVA/I-3 showed no toxic effect for the studied concentrations on the MCF7 tumor line, the normal MeT-5A cell line, and PBMC.

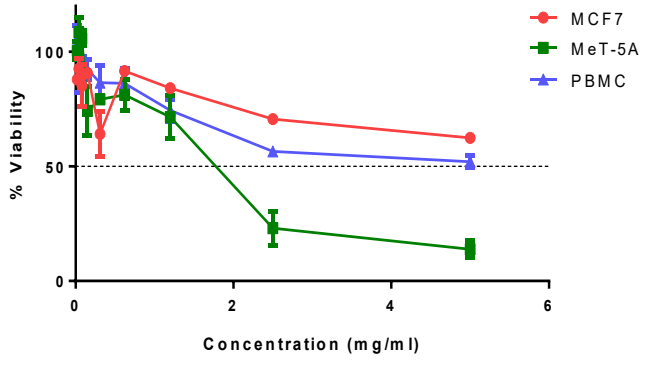

Fig. 6: Cell viability after 48-hour exposure to D/PVA/I-1.

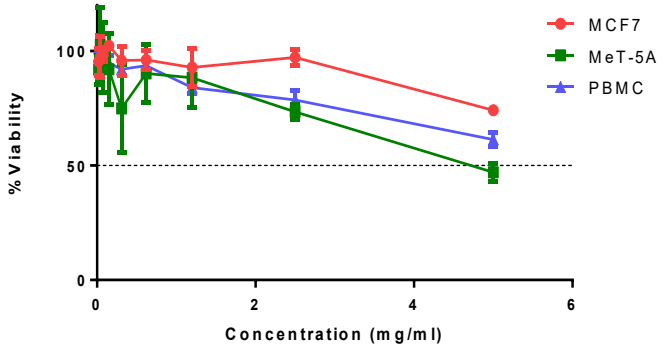

Fig. 7: Cell viability after 48-hour exposure to D/PVA/I-2.

In a comparative analysis of the CAC50 of substances D/PVA/I-1, D/PVA/I-2 and D/PVA/I-3 using Tukey's multiple comparison test, no statistically significant differences were found between the groups (Fig. 8). Although the results suggest a relatively low cytotoxic effect of D/PVA/I-1 and D/PVA/I-2 on the normal MeT-5A cell line and PBMCs, this effect may be influenced by higher than MCF7 tumor line susceptibility.

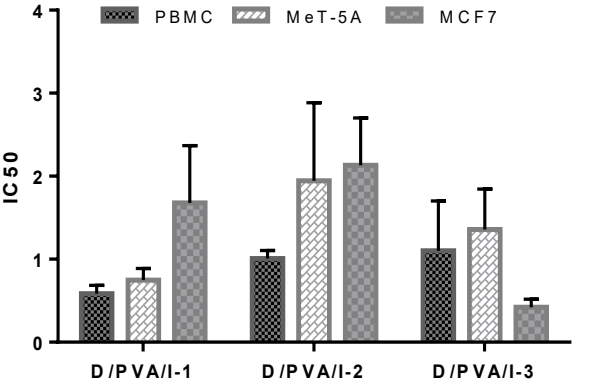

Fig. 8: Comparative analysis of the effect of the studied substances on tumor and normal cell lines and PBMC (CAC50, mean ± SEM; n=4).

4. Conclusion

In this study, dextrin/PVA/iodine (D/PVA/I) complexes were successfully synthesized and structurally characterized using a combination of UV-Vis, FTIR, ^{1}H NMR, XRD, and TG analysis. The antimicrobial performance of these complexes was shown to be influenced by iodine concentration, with D/PVA/I-1 and D/PVA/I-2, which contain higher iodine levels, demonstrating greater efficacy against both Gram-positive and Gram-negative bacteria. However, the relationship between iodine content and bactericidal activity is not strictly linear and appears to vary depending on the bacterial strain. For instance, *Pseudomonas aeruginosa* exhibited tolerance to high iodine levels, suggesting the presence of resistance mechanisms that warrant further investigation.

The study also assessed the cytotoxic effects of the complexes. While D/PVA/I-1 and D/PVA/I-2 showed moderate cytotoxicity toward normal MeT-5A cells at high concentrations, their toxicity toward peripheral blood mononuclear cells (PBMCs) was relatively low, indicating a potential safety margin for biomedical applications. These findings underscore the importance of dose optimization to balance antimicrobial efficacy with biocompatibility. From a practical standpoint, the D/PVA/I complexes-particularly the higher iodine formulations-show promise for clinical and industrial applications, such as in wound care, antiseptic coatings, and disinfectant formulations. Nevertheless, further preclinical and clinical studies are required to fully assess their long-term safety, stability, and effectiveness in real-world conditions. Additionally, future works should focus on tailoring the formulations to overcome bacterial resistance and to minimize potential cytotoxic effects.

Acknowledgements

The authors would like to thank the control and analytical laboratory of SCAID for assisting in preparing the materials

for the article. This research has been/was/is funded by the Committee of Science of the Ministry of Science and Higher Education of the Republic of Kazakhstan (Grant No. BR24992760).

Conflict of Interest

There is no conflict of interest.

Supporting Information

Applicable.

Reference

[1] Z. Zhang, B. Weng, Z. Hu, Z. Si, L. Li, Z. Yang, Y. Cheng, Chitosan-iodine complexes: Preparation, characterization, and antibacterial activity, *International Journal of Biological Macromolecules*, 2024, **260**, 129598, doi: 10.1016/j.ijbiomac.2024.129598.

[2] E. Lamei, M. Hasanzadeh, Fabrication of chitosan nanofibrous scaffolds based on tannic acid and metal-organic frameworks for hemostatic wound dressing applications, *International Journal of Biological Macromolecules*, 2022, **208**, 409-420, doi: 10.1016/j.ijbiomac.2022.03.117.

[3] G. Tao, R. Cai, Y. Wang, L. Liu, H. Zuo, P. Zhao, A. Umar, C. Mao, Q. Xia, H. He, Bioinspired design of AgNPs embedded silk sericin-based sponges for efficiently combating bacteria and promoting wound healing, *Materials & Design*, 2019, **180**, 107940, doi: 10.1016/j.matdes.2019.107940.

[4] D. C. Nwobodo, M. C. Ugwu, C. O. Anie, M. T. S. Al-Ouqaili, J. C. Ikem, U. V. Chigozie, M. Saki, Antibiotic resistance: The challenges and some emerging strategies for tackling a global menace, *Journal of Clinical Laboratory Analysis*, 2022, **36**, e24655, doi: 10.1002/jcla.24655.

[5] F. Prestinaci, P. Pezzotti, A. Pantosti Antimicrobial resistance: a global multifaceted phenomenon. *Pathog Glob Health*, 2015,**109**, 309-18. doi: 10.1179/2047773215Y.0000000030.

[6] N. Jawad Hadi, A. Jabbar Braihi, S. Kareem Mohammed, Effect of flow behavior on the production of PVA/dextrin microspheres, *International Journal of Engineering & Technology*, 2018, **7**, 669-675, doi: 10.14419/ijet.v7i4.19.27979.

[7] A. Qiu, Y. Wang, G. Zhang, H. Wang, Natural polysaccharide-based nanodrug delivery systems for treatment of diabetes. *Polymers (Basel)*, 2022, **8**, 3217. doi: 10.3390/polym14153217.

[8] Bu. Xiaotong, Ji. Na, L. Dai, D. Xuyan, M. Chen, L. Xiong, S. Qingjie, Self-assembled micelles based on amphiphilic biopolymers for delivery of functional ingredients, *Trends in Food Science & Technology*, 2021, **114**, 386-398, doi: 10.1016/j.tifs.2021.06.001.

[9] S. Kotova, S. Kostjuk, Y. Rochev, Y. Efremov, A. Frolova, P. Timashev, Phase transition and potential biomedical applications of thermoresponsive compositions based on polysaccharides, proteins and DNA: A review, *International Journal of Biological Macromolecules*, 2023, **249**, 126054, doi: 10.1016/j.ijbiomac.2023.126054.

[10] H. Lu, Y. Liu, Y. Yang, L. Li, Preparation of poly (vinyl alcohol)/gelatin composites *via in situ* thermal/mechanochemical degradation of collagen fibers during melt extrusion: effect of extrusion temperature, *Journal of Polymer Research*, 2017, **24**, 203, doi: 10.1007/s10965-017-1377-2.

[11] M. I. Baker, S. P. Walsh, Z. Schwartz, B. D. Boyan, A review of polyvinyl alcohol and its uses in cartilage and orthopedic applications, *Journal of Biomedical Materials Research Part B-applied Biomaterials*, 2012, **100**, 1451-1457, doi: 10.1002/jbm.b.32694.

[12] S. D. Yoon, M. H. Park, H. S. Byun, Mechanical and water barrier properties of starch/PVA composite films by adding nano-sized poly(methyl methacrylate-co-acrylamide) particles, *Carbohydrate Polymers*, 2012, **87**, 676-686, doi: 10.1016/j.carbpol.2011.08.046.

[13] R. D. Wolcott, R. G. Cook, E. Johnson, C. E. Jones, J. P. Kennedy, R. Simman, K. Woo, D. Weir, G. Schultz, M. H. Hermans, A review of iodine-based compounds, with a focus on biofilms: results of an expert panel, *Journal of Wound Care*, 2020, **29**, S38-S43, doi: 10.12968/jowc.2020.29.Sup7.S38.

[14] M. López-Álvarez, H. Ulmer, N. Klay, J. M. van Dijl, New *In situ*-generated polymer-iodine complexes with broad-spectrum antimicrobial activity, *Microbiology Spectrum*, 2022, **10**, e0055022, doi: 10.1128/spectrum.00550-22.

[15] Y. Wang, W. Teng, Z. Zhang, S. Ma, Z. Jin, X. Zhou, Y. Ye, C. Zhang, Z. Gou, X. Yu, Z. Ye, Y. Ren, Remote eradication of bacteria on orthopedic implants *via* delayed delivery of polycaprolactone stabilized polyvinylpyrrolidone iodine, *Journal of Functional Biomaterials*, 2022, **13**, 195, doi: 10.3390/jfb13040195.

[16] C. Abueva, H. S. Ryu, J. W. Min, P. S. Chung, H. S. You, M. S. Yang, S. H. Woo, Quaternary ammonium N, N, N-trimethyl chitosan derivative and povidone-iodine complex as a potent antiseptic with enhanced wound healing property, *International Journal of Biological Macromolecules*, 2021, **182**, 1713-1723, doi: 10.1016/j.ijbiomac.2021.05.153.

[17] J. Yu, P. Wang, M. Yin, K. Zhang, X. Wang, B. Han, Carboxymethyl chitosan-grafted polyvinylpyrrolidone-iodine microspheres for promoting the healing of chronic wounds, *Bioengineered*, 2022, **13**, 8735-8746, doi: 10.1080/21655979.2022.2054911.

[18] Y. Chen, H. Qiu, M. Dong, B. Cheng, Y. Jin, Z. Tong, P. Li, S. Li, Z. Yang, Preparation of hydroxylated lecithin complexed iodine/carboxymethyl chitosan/sodium alginate composite membrane by microwave drying and its applications in infected burn wound treatment, *Carbohydrate Polymers*, 2019, **206**, 435-445, doi: 10.1016/j.carbpol.2018.10.068.

[19] L. Zhang, Z. Zhang, C. Li, Z. Hu, Y. Liang, Z. Yang, Y. Cheng, D. Huang, Preparation and characterization of amphiphilic chitosan/iodine composite film as antimicrobial material, *International Journal of Biological Macromolecules*, 2022, **222**, 2426-2438, doi: 10.1016/j.ijbiomac.2022.10.028.

[20] D. N. Makhayeva, G. S. Irmukhametova, V. V. Khutoryanskiy, Polymeric iodophors: preparation, properties, and biomedical applications, *Review Journal of Chemistry*, 2020, **10**, 40-57, doi: 10.1134/S2079978020010033.

[21] A. Telfah, Q. M. Al-Bataineh, E. Tolstik, A. A. Ahmad, A. M. Alsaad, R. Ababneh, C. J. Tavares, R. Hergenröder, Optical, electrical and chemical properties of PEO: I2 complex composite films, *Polymer Bulletin*, 2023, **80**, 9611-9625, doi: 10.1007/s00289-022-04508-4.
[22] S. Pesek, R. Silaghi-Dumitrescu, The iodine/iodide/starch supramolecular complex, *Molecules*, 2024, **29**, 641, doi: 10.3390/molecules29030641.
[23] K. Tashiro, Structural views of Electrically-conductive polymers, structural science of crystalline polymers, microscopically-viewed structure-property relationship, Springer, Singapore, 2024, 627-712, ISBN 978-981-99-5260-1.
[24] S. Moulay, Macromolecule/polymer-iodine complexes: an update, *Recent Innovations in Chemical Engineering*, 2019, **12**, 174-233, doi: 10.2174/2405520412666190716163611.
[25] S. T. Kenesheva, S. Taukobong, S. V. Shilov, T. V. Kuznetsova, A. B. Jumagaziyeva, T. A. Karpenyuk, O. N. Reva, A. I. Ilin, The Effect of Three Complexes of Iodine with Amino Acids on Gene Expression of Model Antibiotic Resistant Microorganisms Escherichia coli atcc baa-196 and Staphylococcus aureus atcc baa-39, *Microorganisms*, 2023, **11**, 1705, doi: 10.3390/microorganisms11071705.
[26] B. L. Zimmer, D. E. Carpenter, G. Esparza, K. Alby, Broth and agar dilution antimicrobial susceptibility testing process, Methods for Dilution Antimicrobial Susceptibility Tests for Bacteria That Grow Aerobically, CLSI, 2024, 118, ISBN: 978-1-68440-226-7.
[27] James S. Lewis II, supplement M100, Performance standards for antimicrobial susceptibility testing, CLSI, 2025, 428, ISBN: 978-1-68440-262-5.
[28] T. Mosmann, Rapid colorimetric assay for cellular growth and survival: Application to proliferation and cytotoxicity assays, *Journal of Immunological Methods*, 1983, **65**, 55-63, doi: 10.1016/0022-1759(83)90303-4.
[29] Z. Chen, L. Zhu, T. Song, J. Huang, Y. Han, Determination of dextrin based on its self-aggregation by resonance light scattering technique, *Analytica Chimica Acta*, 2009, **635**, 202-206, doi: 10.1016/j.aca.2009.01.002.
[30] M. Sai, R. Guo, L. Chen, N. Xu, Y. Tang, D. Ding, Research on the preparation and character- ization of chitosan grafted polyvinylpyrrolidone gel membrane with iodine, *Journal of Applied Polymer Science*, 2015, **132,** 41797. doi.org/10.1002/app.41797.
[31] P. K. Weisseborn, L. J. Warren, J. G. Dunn, Selective flocculation of ultrafine iron ore. 1. Mechanism of adsorption of starch onto hematite, *Colloids and Surfaces A*: *Physicochemical and Engineering Aspects*, 1995, **99**, 11-27, doi: 10.1016/0927-7757(95)03111-P.
[32] L. O. Filippov, V. V. Severov, I. V. Filippova, Mechanism of Starch Adsorption on Fe-Mg-Al-bearing Amphiboles, *The International Journal of Mineral Processing*, 2013, **123**, 120-128, doi: 10.1016/j.minpro.2013.05.010.
[33] B. Kar, H. Sahoo, S. S. Rath, B. Das, Investigations on different starches as depressants for iron ore flotation, *Minerals Engineering*, 2013, **49**, 1-6, doi: 10.1016/j.mineng.2013.05.004.
[34] S. Pavlovic, P. R. G. Brandao, Adsorption of starch, amylose, amylopectin and glucose monomer and their effect on the flotation of hematite and quartz, *Minerals Engineering*, 2003, **16**, 1117-1122, doi: 10.1016/j.mineng.2003.06.011.
[35] A. A. El-Midany, Y. Arafat, T. F. El-Faris, Rice starch as a depressant in phosphate reverse flotation, *Starch-Stärke*, 2015, **67**, 745-751. doi.org/10.1002/star.201500049.
[36] W. Qin, Q. Wei, F. Jiao, C. Yang, R. Liu, P. Wang, L. Ke, Utilization of polysaccharides as depressants for the flotation separation of copper/lead concentrate, *International Journal of Mining Science and Technology*, 2013, **23**, 191-198.
[37] G. M. Lampman, G. S. Kriz, J. R. Vyvyan, infrared spectroscopy, Introduction to Spectroscopy, fifth editiona, Washington, 2013, 34-126, ISBN: 978-1-285-46012-3.
[38] N. V. Bhat, M. M. Nate, M. B. Kurup, V. A. Bambole, S. Sabharwal, Effect of γ-radiation on the structure and morphology of polyvinyl alcohol films, *Nuclear Instruments and Methods in Physics Research Section B*, 2005, **237**, 585-592, doi: 10.1016/j.nimb.2005.04.058.
[39] J. Lee, T. Isobe, M. Senna, Preparation of ultrafine Fe_3O_4 particles by precipitation in the presence of PVA at high pH, *Journal of Colloid and Interface Science*, 1996, **177,** 490-494, doi.org/10.1006/jcis.1996.0062.
[40] I. Omkaram, R. P. Sreekanth Chakradhar, J. Lakshmana Rao, EPR, optical, infrared and Raman studies of VO_2^+ ions in polyvinylalcohol films, *Physica B*: *Condensed Matter*, 2007, **388**, 318-325, doi: 10.1016/j.physb.2006.06.134.
[41] X. Lan, W. Li, C. Ye, L. Boetje, T. Pelras, F. Silvianti, Q. Chen, Y. Pei, K. Loos. Scalable and Degradable Dextrin-Based Elastomers for Wearable Touch Sensing. *ACS Applied Materials & Interfaces*, 2023, **25**, 4398-4407, doi: 10.1021/acsami.
[42] A. Radoń, P. Włodarczyk, Influence of water on the dielectric properties, electrical conductivity and microwave absorption properties of amorphous yellow dextrin, *Cellulose*, 2019, **26**, 2987-2998, doi: 10.1007/s10570-019-02324-0.
[43] J. Sun, R. Zhao, J. Zeng, G. Li, X. Li, Characterization of dextrins with different dextrose equivalents, *Molecules*, 2010, **15**, 5162-5173, doi: 10.3390/molecules15085162.
[44] S. B. Aziz, Modifying poly(vinyl alcohol) (PVA) from insulator to small-bandgap polymer: a novel approach for organic solar cells and optoelectronic devices, *Journal of Electronic Materials*, 2016, **45**, 736-745, doi: 10.1007/s11664-015-4191-9.
[45] O. G. Abdullah, S. B. Aziz, M. A. Rasheed, Structural and optical characterization of PVA: $KMnO_4$ based solid polymer electrolyte, *Results in Physics*, 2016, **6**, 1103-1108, doi: 10.1016/j.rinp.2016.11.050.
[46] O. N. Reva, I. S. Korotetskiy, M. Joubert, S. V. Shilov, A. B. Jumagaziyeva, N. A. Suldina, A. I. Ilin, The effect of iodine-containing nano-micelles, FS-1, on antibiotic resistance, gene expression and epigenetic modifications in the genome of multidrug resistant MRSA strain *Staphylococcus aureus* ATCC BAA-39, *Frontiers in Microbiology*, 2020, **11**, 581660, doi: 10.3389/fmicb.2020.581660.

[47] A. M. Salisbury, M. Mullin, L. Foulkes, R. Chen, S. L. Percival, Controlled-release iodine foam dressings demonstrate broad-spectrum biofilm management in several *in vitro* models, *International Wound Journal*, 2022, **19**, 1717-1728, doi: 10.1111/iwj.13773.
[48] E. Pedrotti, E. Bonacci, R. Kilian, C. Pagnacco, A. Fasolo, M. Anastasi, G. Manzini, F. Bosello, G. Marchini, The role of topical povidone-iodine in the management of infectious keratitis: a pilot study, *Journal of Clinical Medicine*, 2022, **11**, 848, doi: 10.3390/jcm11030848.
[49] K. Reimer, T. A. Wichelhaus, V. Schäfer, P. Rudolph, A. Kramer, P. Wutzler, D. Ganzer, W. Fleischer, Antimicrobial effectiveness of povidone-iodine and consequences for new application areas, *Dermatology*, 2002, **204**, 114-120, doi: 10.1159/000057738.
[50] Y. Cheng, T. Lin, Y. Pan, Y. Wang, Y. Lin, J. Wang, Colistin resistance mechanisms in Klebsiella pneumoniae strains from Taiwan. *Antimicrob Agents Chemother*, 2015 **59**, 2909-2913, doi: 10.1128/AAC.04763-14.
[51] A. Elfadadny, R. F. Ragab, M. AlHarbi, F. Badshah, E. Ibáñez-Arancibia, A. Farag, A. O. Hendawy, P. R. De los Ríos-Escalante, M. Aboubakr, S. A. Zakai, W. M. Nageeb, Antimicrobial resistance of pseudomonas aeruginosa: navigating clinical impacts, current resistance trends, and innovations in breaking therapies, *Frontiers in Microbiology*, 2024, **15**, 1374466, doi: 10.3389/fmicb.2024.1374466.
[52] M. Fernández-Billón, A. E. Llambías-Cabot, E. Jordana-Lluch, A. Oliver, M, D Macià, Mechanisms of antibiotic resistance in *Pseudomonas aeruginosa* biofilms, *Biofilm*, 2023, **5**, 100129, doi: 10.1016/j.bioflm.2023.100129.
[53] M. Pichon, C. Burucoa, V. Evplanov, F. Favalli, Efficacy of three povidone iodine formulations against *Cutibacterium acnes* assessed through In vitro studies: A preliminary study, *Antibiotics*, 2022, **11**, 665, doi: 10.3390/antibiotics11050665.
[54] B. A. Saggers, G. T. Stewart, Polyvinyl-pyrrolidone-iodine: an assessment of antibacterial activity, *Epidemiology and Infection*, 1964, **62**, 509-518, doi: 10.1017/s0022172400040225.
[55] M. Ignatova, N. Markova, N. Manolova, I. Rashkov, Antibacterial and antimycotic activity of a cross-linked electrospun poly(vinyl pyrrolidone)-iodine complex and a poly(ethylene oxide)/poly(vinyl pyrrolidone)-iodine complex, *Journal of Biomaterials Science*, *Polymer Edition*, 2008, **19**, 373-386, doi: 10.1163/156856208783721056.
[56] F. Watson, R. Chen, S. L. Percival, *In vitro* prevention and inactivation of biofilms using controlled-release iodine foam dressings for wound healing, *International Wound Journal*, 2024, **21**, e14365, doi: 10.1111/iwj.14365.